Analysis of time-lapse logs to determine shale-related R factor

Citation for published version:
Jaramillo, A, Mangriotis, M-D & MacBeth, C 2018, 'Analysis of time-lapse logs to determine shale-related R factor', *SEG Technical Program Expanded Abstracts*, pp. 5357-5361. https://doi.org/10.1190/segam2018-2996009.1

Digital Object Identifier (DOI):
10.1190/segam2018-2996009.1

Link:
Link to publication record in Heriot-Watt Research Portal

Document Version:
Peer reviewed version

Published In:
SEG Technical Program Expanded Abstracts

Analysis of time-lapse logs to determine shale-related R factor

Alejandro Jaramillo, Maria-Daphne Mangriotis and Colin MacBeth, Heriot-Watt University*

Summary

Time-lapse changes in the overburden can be related to pore pressure variations in the underlying reservoir. The geomechanical changes observed are independent of fluid flow given the impermeable nature of the caprock, however, such deformation has the potential of causing a significant impact on the 4D signal. A physical model widely used to couple geomechanics and time-lapse seismic signatures, relates the fractional change in velocity and the vertical strain of reservoir and surrounding rocks via a constant factor *R*. This study presents improvements in understanding and predictability of the overburden *R* factors for future seismic interpretation. Here, we compare two different methods to investigate the complexity of the *R* factors using the well log data of two Jurassic shales from Central North Sea. A time-lapse analysis on repeated well logs is carried out to reveal the velocity response to porosity and pressure change that results into dilation in the overburden. The results are compared to estimates from a theoretical model that describes the unloading process in shales.

Introduction

It is commonplace in geomechanical simulations to regard the strata overlying the reservoir as homogeneous sequences. Whilst this simplification seems to be acceptable in some cases, several published field cases indicate that during production, pore pressure reduction in the reservoir generates strain deformation in the overburden that varies with lithology and stress path. Particularly, overburden shales play a significant role acting as seals that prevent hydrocarbons to escape from the reservoir due to their low permeability and capillary sealing (Johnston and Christensen, 1995). In terms of seismic wave propagation, shale rocks can be highly anisotropic (Sayers 2006). The phenomenon of geomechanical activation of the overburden shales is more significant in high pressure and high temperature (HP/HT) fields due to larger differences in pore pressure measured after production (Figure 1). In some cases, the aforementioned overburden strain has also caused the failure of production wells due to a significant weakening of the shale caprock increasing the operational risk of drilling new wells in such a challenging environment (De Gennaro et al., 2017). The geomechanical response is also present in 4D seismic surveys as a time-shift variation following the velocity perturbation. Time-shifts represent a primary source of indirect information on reservoir and surrounding rocks deformation; their relationship to strain and velocity change is shown in eq. 1. In addition, an empirical solution to convert time-shifts to geomechanical strain was proposed by Hatchell and Bourne (2005) and Røste et al. (2005) with a physical model (HBR model) that couples velocity perturbations with vertical strain via a constant factor *R* (eq. 2).

$$\Delta t = \int_0^T \left(\varepsilon_{zz} - \frac{\Delta V}{V} \right) dt \qquad (1)$$

and

$$\frac{\Delta V}{V} = -R\varepsilon_{zz} \qquad (2)$$

where: Δt is the time-shift, ε_{zz} is the vertical strain and ΔV is the change in velocity.

The definition of *R* has been described in the literature as a characteristic property of the rock where both the subsurface and vertical strain are assumed to be homogenous and responding primarily to a relative change in vertical velocities mainly affected by porosity and/or fluid variations during reservoir depletion or inflation (Holt et al., 2008). To date, *R* values have been published for a wide range of reservoirs and overburden rocks. MacBeth et al. (2018a) provided a list of *R* factors from different fields, concluding that *R* values between 5 and 20 are commonly found in the overburden. Also, laboratory tests in sedimentary rocks suggest *R* factors are sensitive to stress orientation, magnitude and lithology, yielding larger *R* factors than those derived from field observation (Holt et al., 2008).

This study aims at computing shale *R* factors from a repeated well log analysis. It then uses a micro-mechanical deformation model to interpret these values for shales. In both cases we consider geological and petrophysical properties of two units from a HP/HT North Sea field, corresponding to the Jurassic Heather and Kimmeridge Clay Formations.

R-factor measurement based on repeated well logs

The repeated well logs consist of a baseline (main well) and monitor (sidetrack well, with offset less than 100m) drilled over a period of two years. During that time, the reservoir experienced substantial pore pressure decline (~3500psi). Available logs for our analysis include gamma ray (GR), neutron, density, sonic, and spectral gamma ray, which include records within the reservoir and overburden shales (Figure 1). The strength of having time-lapse log analysis for R factor estimation is that it permits direct estimation of R via eq. (2) using $\Delta V / V$ estimate from time-lapse sonic logs and vertical strain computed directly from changes in formation thickness or indirectly from changes in time-lapse porosity values. We first perform a petrophysical analysis of gamma ray (GR), sonic and density logs for the two repeated logs to establish a predictive model from rock properties. The methodology takes into account:

a. Statistics for quality control: The aim of the quality control and statistical analysis is two-fold: firstly to assess borehole conditions, deviation survey and vertical corrections, noise spikes and cycle skipping. To this end, we perform Kolmogorov-Smirnov test on the cumulative fractions of the GR logs from both wells, and find small statistic D-values (< 0.114), and, in addition, large Pearson correlation factors (r=0.850) in the reservoir formations, which are both indicative of good correlation between baseline and monitor logs. On the other hand, the overburden shale formations show larger variations between the baseline and monitor logs (r=0.604). Secondly, we assess the differences between overburden shales and reservoir formations in the baseline and monitor wells. Figure 2 shows cross-plots of porosity versus P-wave velocity for the baseline and monitor wells, showing separated clusters for the Lower/Upper Fulmar, Heather and Kimmeridge formations (shown in Figure 3) and verify a linear relationship of sonic velocity to density.

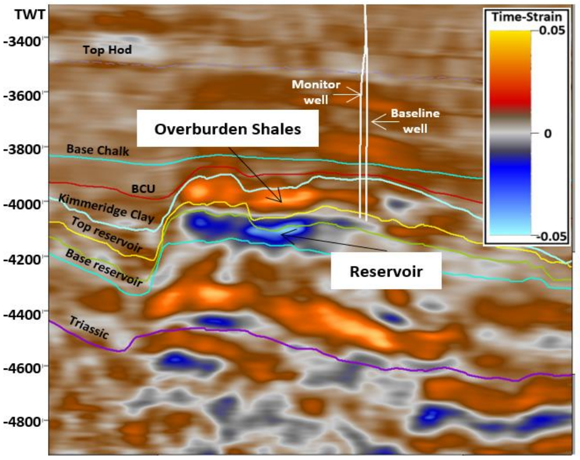

Figure 1: Time-strains between 2001-13 in a North-Sea field. baseline and monitor wells were drilled between 2000 - 2002 with a reduction in pore pressure of approximately 3500 psi.

b. Cyclicity analysis to detect repeated stratigraphic patterns in GR and density logs. We assess the cyclicity of the Upper Jurassic units (Upper Fulmar, Heather and Kimmerdige clay formations) by comparing the baseline/monitor wells against four additional wells at larger offsets (up to 400m) to help determine if the lateral distance between them has a significant effect on their log response. Our comparison of Fourier spectrum and continuous wavelet transforms suggests increased correlation over shorter distances with minor effects in log response cyclicity between baseline/monitor wells.

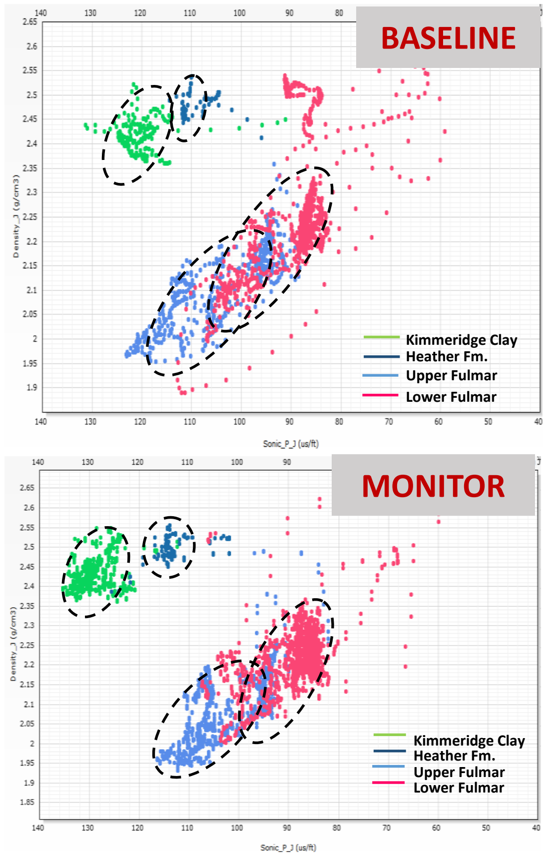

Figure 2: Cross-plot for Kimmeridge, Heather and Upper/Lower Fulmar formations for sonic versus density.

c. Relationship between time-lapse petrophysics and geomechanics via *R* factor estimation. After assessing the statistics and cyclicity of the repeated logs and aligning the logs using vertical projection methods, we first attempt to compute vertical strain from the repeated GR logs, by assessing thickness changes between each well, within each formation. We first consider strain estimates based on geological tops as well as interpreted internal geological picks. Although strains computed show compaction in the reservoir and expansion in the overburden, the magnitudes of computed strains are roughly 1-2 orders of magnitude higher than the expected strains. Our conclusion is that strain estimation via direct measurement of thickness changes of formations between the two logs is unreliable. The most probable explanation is that lateral differences in thicknesses, both due to differential erosion and shear faulting, are too large to extrapolate meaningful strain estimates.

Next, we compute total porosity to assess time-lapse changes in the Heather and Kimmeridge Clay in response to reservoir depletion (Figure 3). To this end, we test two methods for porosity calculation, firstly the neutron-density porosity method, and secondly the time average method. The first method gives unreliable porosity estimates (in fact showing a reduction in porosity in overburden shales after depletion in reservoir), which may have been due to varying logging tool responses being not adequately corrected for environmental factors such as hole size, mud density etc. The second method, yields changes of porosity that are in line with an expanding overburden and compacting reservoir. Lastly, based on the assumption that the vertical strain is proportional to a differential change in porosity, we compute *R* factors for the overburden shales:

$$R = -\frac{\Delta V}{V} / \frac{\Delta\phi}{(1-\phi)} \tag{3}$$

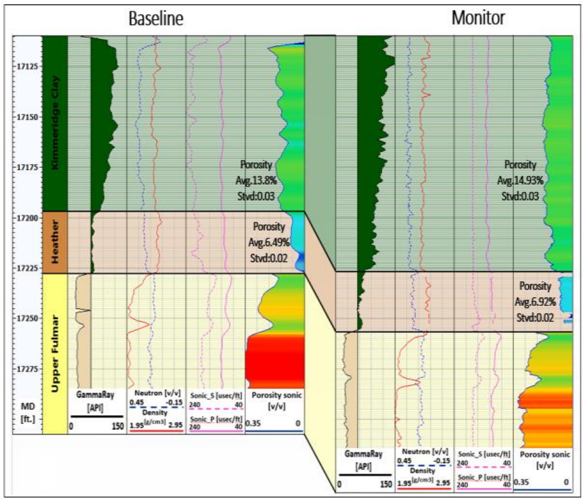

Figure 2: Section showing gamma ray, neutron density, P-S sonic and calculated porosity logs for the baseline and monitor wells.

Using eq. (3), we run 100,000 random Monte Carlo computations to predict normal distributions of porosity and the change in velocities from logs. The results show a mean $R \approx 4.8$ (range 5.3-8.7) for the Heather Fm. and $R \approx 5.3$ (range 3-7.4) for the Kimmeridge Clay. Figure (4) shows the sonic P-wave versus porosity computed from logs and suggests part of the velocity change is accompanied by porosity change, even for high volume of clay content. It should be noted that our computed R values are in agreement with published values from seismic observations in the overburden (as previously mentioned, those range from 5-20), and can be potentially explained via a porosity-dependent R factor such as the Xu and White (1995) model, which considers the pore volume built from combination of sand- and shale-related pores. As shown in MacBeth (2018b), for a sandy shale, the Xu and White (1995) model yields an R factor of 6. However a study conducted by Katahara (2017) on the clay effect in shale velocity suggests that the strong variation of velocity with clay content is not due to porosity variations, but clay mineral concentration and orientation as clays become denser with depth. Following this statement, we can infer that if velocity is not solely controlled by porosity, then consequently the *R* factor should be related to additional properties such as small-scale micro-damage, clay content or mineral orientation.

R-factor model for shales

The model of shales required to characterize lithology-dependent *R* factors, considers two elements: firstly, an understanding of shale anisotropy; and secondly, a plausible physical model for the contact regions between clay platelets. To this end, we consider that shales are transversely isotropic with a vertical axis of symmetry (VTI), and can be represented by the Thomsen's parameters (ε, δ and γ) and the vertical P-wave and S-wave velocities (VP0, VS0) taken from the repeated well sonic logs. The anisotropy is largely determined by the mineralogical composition, maturity (kerogen content) and alignment of minerals. The minerology and organic content for both the Heather and Kimmeridge shales is characterized based on spectral gamma ray analysis to identify the dominant clay mineral and organic content. Following this procedure, illite is identified as the most dominant mineral at proportions 39% for Heather Fm. and 45% for Kimmeridge Clay. To calculate the total organic content (TOC) in the Kimmeridge Clay we apply two methods: the Uranium and the density techniques resulting in 2.5% average concentration, which agrees with the published TOC values in the Central North Sea for the organic shale (Fishman et al., 2012). Similarly, we assess the impact of silt inclusion on the fabric orientation and anisotropy by correlating our shales with data published by Johnston and Christensen (1995) where the preferred clay mineral orientation and ε and δ Thomsen's parameters are compared against silt content. The correlation suggests that the preferred orientation of illite-rich shales varies with silt content as ε decreases with increasing quartz while δ shows no such correlation.

During production, continuous depletion of the reservoir induces unloading to overburden shales. As a result, the velocity is reduced mainly due to internal damage, whereas porosity could also affect velocity change (Katahara, 2017). With the background set by the VTI described above, we assume that the strain deformation in the overburden is generated by weakening clay platelet/mineral contacts, and that these can be represented by excess compliance as defined by Sayers and Kachanov (1995). Their conceptual model, combined with derivations from MacBeth et al. (2018b) is used to generate the velocity changes and R-factors that we see in our data.

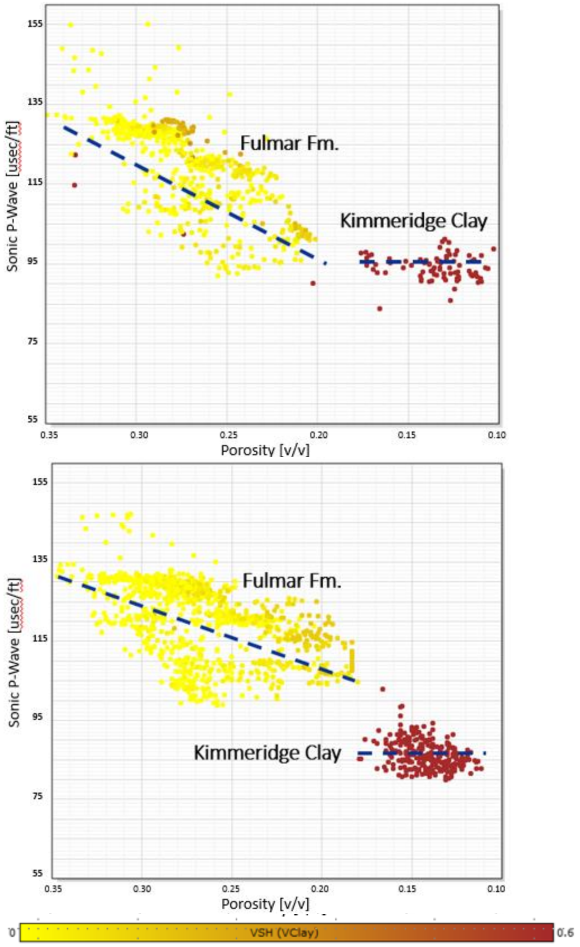

Figure 4: Cross-plot showing sonic P-wave velocity versus porosity for aseline (top) and monitor (bottom). Formations are colour-coded based on their clay content.

The relative magnitudes of the resultant *R* factors are computed for the Heather and Kimmeridge Clay as a function of porosity and aspect ratio (Table 1). These ratios represent the extremes of the accepted distribution from published work, for which α values lie between 0.001 and 0.1. The *R* factors are found to be larger for the more anisotropic Kimmeridge Clay than for the Heather Fm. and in both cases increase when the aspect ratio decreases. The higher *R* factors found in the overburden shales are the result of the compliant nature of this lithology, suggesting that the mechanism of contact disengagement between clay platelets is an efficient generator of large values. Such high values could signal that shale intervals have failed significantly, leading to mechanical instability of the caprock. However, the required aspect ratio to obtain R values within 5 are in the order of 0.2 which is considered unrealistic.

Table 1: *R*-values for Kimmeridge Clay and Heather Formation from the micromechanical model proposed. Four aspect ratios and a background VTI medium are considered for calculations.

Unit	**Lithology**	**α** *(Aspect ratio)*	**Ø** *(Porosity)*	**R^+** *(R-Factor)*
Kimmeridge Clay	*Organic black shales*	0.001	*0.138*	*344*
		0.01	*0.138*	*218*
		0.035	*0.138*	*114*
		0.1	*0.138*	*53*
Heather	*Marine shales and ssts.*	0.001	*0.065*	*108*
		0.01	*0.065*	*90*
		0.035	*0.065*	*63*
		0.1	*0.065*	*36*

Conclusions

Petrophysical analysis of repeated wireline logs has shown that R-factors of around 5 are appropriate for both the Heather and Kimmeridge clay based on an HBR model using log-derived time-lapse porosity values. This range is in agreement with most published overburden R values from seismic data, and can be explained by porosity deformation. It is known that internal damage can lead to the elevated R factors that we occasionally observe in the overburden, however, we believe that this effect is secondary in the formations we are investigating.

Acknowledgements

We thank the sponsors of the Edinburgh Time-Lapse Project, Phase VI (AkerBP, BP, CGG, Chevron, ConocoPhillips, ENI, ExxonMobil, Hess, Landmark, Maersk, Nexen, Norsar, OMV, PGS, Petrobras, Shell, Statoil and Taqa) for supporting this research. We are grateful to Jonathan Brain and Erick Alvarez for helpful discussions on this research, and Shell UK for permission to present these data.